Available online at www.sciencedirect.com
ScienceDirect
Acta Materialia 55 (2007) 295–300
Acta MATERIALIA
www.actamat-journals.com

Effect of the nanoindentation rate on the shear band formation in an Au-based bulk metallic glass

B. Yang [a], T.G. Nieh [a,b,*]

[a] *Materials and Technology Division, Oak Ridge National Lab, Oak Ridge, TN 37831, USA*
[b] *Department of Materials Science and Engineering, The University of Tennessee, TN 37996, USA*

Received 19 July 2006; received in revised form 3 August 2006; accepted 8 August 2006
Available online 3 November 2006

Abstract

This study investigated the nanoindentation behavior of $Au_{49}Ag_{5.5}Pd_{2.3}Cu_{26.9}Si_{16.3}$ bulk metallic glass samples at loading rates ranging from 0.03 to 300 mN s^{-1}. Notable shear band pop-in events were observed. The pop-in size was observed to increase linearly with the load and decreased exponentially with the strain rate. A free-volume mechanism was proposed for interpreting these observations quantitatively. The results and analyses also shed light on the shear band nucleation and evolution processes in bulk metallic glasses.

Keywords: Metallic glasses; Plastic deformation; Hardness; Deformation inhomogeneities

1. Introduction

Bulk metallic glasses have aroused extensive interest in recent years because of their superior structural properties, such as ultra-high strength, a large elastic limit and high wear resistance [1–6]. The lack of line and planar defects in their amorphous structure, such as dislocations and grain boundaries, results in bulk metallic glasses with superior strength over their crystalline counterparts. However, their high strength is also accompanied by brittleness caused by highly localized shear band deformation, which greatly limits the applications of bulk metallic glasses.

Several recent efforts have been made at studying their shear band evolution patterns after monotonic loading experiments [7,8]. It was observed that the shear band size and density varied with the applied strain rate. However, in a deformed bulk metallic glass, the region of deformed shear bands is expected to be softer than that of non-deformed shear bands. As a result, it is possible for shear bands to initiate repeatedly from already weakened locations during these experiments. This phenomenon complicates postmortem micro-structural analysis, because a shear band observed under scanning electron microscopy/transmission electron microscopy may be a result of multiple shear band initiations at the same location. Thus, the size and density of the observed shear bands could not be directly correlated with shear band nucleation and evolution patterns.

Some state-of-the-art in situ characterization methods, e.g. nanoindentation and thermographic detection, have been used for probing the time and spatial arrangements of shear bands during the deformation of bulk metallic glasses [9–13]. The excellent time and displacement resolution of a nanoindenter, for instance, has been demonstrated in the analysis of shear band evolution [11–13]. Schuh et al. [11,12] recently studied the shear band pop-in phenomenon under different load, strain rate and temperature conditions using a Triboindenter®. They also successfully applied the free-volume theory for explaining the observed shear band evolution patterns. However, it is noted that the fruitful amount of pop-in data obtained from nanoindentation tests has not been fully analyzed. Thus, the goal of this paper was

* Corresponding author. Address: Department of Materials Science and Engineering, The University of Tennessee, TN 37996, USA.
E-mail address: tnieh@utk.edu (T.G. Nieh).

1359-6454/$30.00
doi:10.1016/j.actamat.2006.08.028

to extend the previous analyses of the pop-in size and distribution under various loads and strain rates. The analyses were then used for disclosing the nature of free-volume evolution, which controls the nucleation and propagation of localized shear bands.

2. Experimental methods

The bulk metallic glass material used in the present study was $Au_{49}Ag_{5.5}Pd_{2.3}Cu_{26.9}Si_{16.3}$, which was recently developed by Schroers et al. [14]. Alloy ingots of 3 mm in diameter were prepared by arc melting a mixture of elements with purities of >99.8%. X-ray diffraction and differential scanning calorimetry measurements were subsequently performed in order to confirm the amorphous nature of these samples and a glass transition temperature (T_g) of 400 K. The ingots were sliced into coupons with a thickness of 1 mm for nanoindentation experiments. The surfaces of these coupons were polished to a final grit size of 0.03 μm using diamond powders prior to the nanoindentation experiments.

Instrumented nanoindentation experiments were conducted using a Triboindenter® (Hysitron, Inc., Minneapolis, MN). The indenter has a high data acquisition rate of up to 10^4 s^{-1}. The experiments were performed under load control with a maximum load of 5 mN. Loading rates of 0.03, 0.1, 0.3, 1, 3, 10, 30, 100 and 300 mN s^{-1} were applied.

3. Results and discussion

3.1. Pop-in size versus the indentation depth

The *P–h* curve of Au-bulk metallic glass tested under nanoindentation at a loading rate of 0.3 mN s^{-1} at room temperature is plotted in Fig. 1a. A notable pop-in phenomenon was clearly observed. These pop-in steps represented instantaneous shear band bursts and have been previously observed in many other bulk metallic glass systems under nanoindentation [11–13,15–17]. This pop-in phenomenon has been characterized by its size (displacement increment), initiation depth, strain rate and temperature [11–13,17]. One of the distinct observations was that the pop-in size increased with the indentation depth, while the number of pop-in events decreased [11–13]. This was also observed in the present Au-bulk metallic glass, as shown in Fig. 1a. Intuitively, this observation appears to be "a natural consequence of the increasing length scale of the indentation geometry as the depth increases" [12]. However, a physical meaning of this scaling phenomenon has not been offered.

Greer et al. [13] pointed out that the elastic strain increment ($\delta h_e/h$) between two consecutive pop-in events was approximately a constant during nanoindentation of a bulk metallic glass. Here, δh_e is the elastic displacement increment between two pop-in events and h is the indentation depth. Since the elastic strain is proportional to the elastic stress, the elastic stress increment between each two consecutive pop-in events should also be a constant. Furthermore, since a bulk metallic glass behaves like a perfectly plastic material, the yielding strength (or hardness) does not change with the depth and, thus, this stress increment must be balanced out by the same amount of stress drop during a pop-in event. This indicates that all pop-in events were terminated by a similar amount of stress reduction during nanoindentation. This stress reduction is apparently caused by a free-volume increase inside an active shear band. When a shear band is activated, a part of the applied mechanical energy is consumed for creating defects and the free volume inside the shear band. According to the free-volume theory [18–20], a lower threshold stress than the activation stress would be needed for propagating the shear band further and this results in softening of the shear band [7,21]. The amount of stress reduction should follow the statistical distribution of the free volume in shear bands, which is determined by the applied stress, not the load.

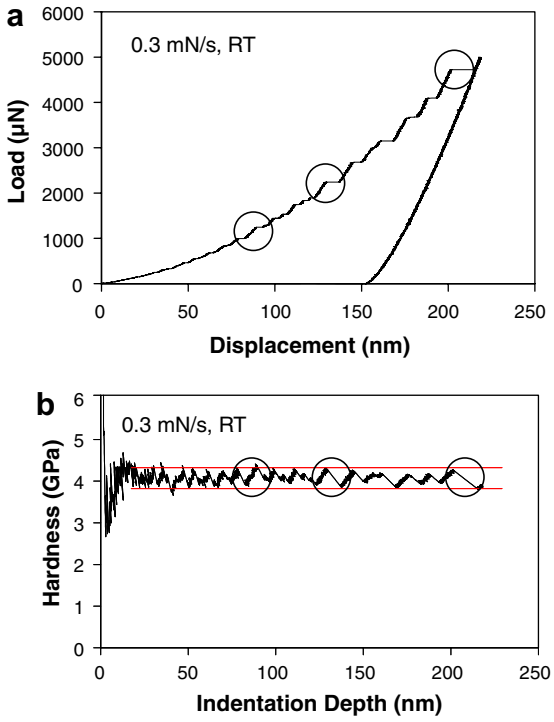

Fig. 1. Observed pop-in events during nanoindentation of an Au-based bulk metallic glass at a constant loading rate of 0.3 mN s^{-1} at room temperature. (a) *P–h* curve and (b) projected curve of the hardness versus indentation depth.

In order to verify this implication, the data in Fig. 1a were re-plotted as the hardness versus indentation depth in Fig. 1b. Note that the hardness is proportional to the stress. Here the hardness H equals P/A, where P is the applied load and A is the indentation area calculated by the area function of the indenter tip [22]. The pop-in steps in Fig. 1a are projected into hardness serrations in Fig. 1b. The hardness reduction (Fig. 1b) at each serration corresponds to a pop-in event (Fig. 1a) and the hardness increase (Fig. 1b) at each serration corresponds to the elastic portion between two pop-in events (Fig. 1a). It is

evident in Fig. 1b that, although the pop-in size varies with the indentation depth in Fig. 1a, the hardness (stress) reduction at each pop-in event is indeed approximately a constant throughout the entire indentation process. It is noted that the hardness serration curve is particularly useful for capturing small pop-in events at shallow indentation depths (20–50 nm), as the hardness reductions at small pop-in events are equally as large as those from large pop-in events.

For an ideal Berkovich indenter tip the area function is $A = 24.5h^2$. At a pop-in event, the load P is constant and the hardness drop ΔH can be calculated as

$$\Delta H = \frac{P}{24.5h^2} - \frac{P}{24.5(h+\Delta h)^2} \quad (1)$$

where Δh is the displacement increment at a pop-in event.

Assuming $\Delta h \ll h$ and rearranging Eq. (1) gives

$$\Delta h = \frac{24.5h^3\Delta H}{2P}. \quad (2)$$

With a Berkovich indenter tip, the loading curve of a monolithic material can be described by a simple power-law relationship [22,23] during nanoindentation:

$$P = K_m h^2 \quad (3)$$

where K_m is a material constant.

Combining Eqs. (2) and (3) gives

$$\Delta h = \frac{24.5\Delta H}{2K_m} h \quad (4)$$

This relationship shows that, when shear band propagation is terminated by a hardness reduction, the pop-in size Δh is expected to increase linearly with the indentation depth. This linear relationship was readily seen in the present study, as shown in Fig. 2. This also explains the "length scaling" phenomenon reported in several previous studies [12,13]. Since the pop-in size increases with the indentation depth, a natural consequence is that fewer pop-in events are needed for the same amount of indentation displacement. This is the reason why the frequency of pop-in events decreases with the indentation depth.

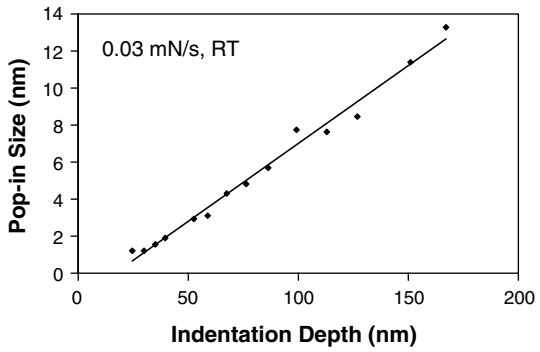

Fig. 2. Measured pop-in size versus the indentation depth for a nanoindentation experiment of an Au-based bulk metallic glass at a constant loading rate of 0.03 mN s^{-1} at room temperature.

3.2. Pop-in size versus the strain rate

The P–h curves of Au-bulk metallic glass at loading rates from 0.03 to 300 mN s^{-1} are shown in Fig. 3a. With the exception of the curve at 0.03 mN s^{-1}, all the other curves are plotted on the same axes with their origins offset 50 nm for clarity of presentation. It is readily seen in Fig. 3a that the most significant pop-in event occurs at the slowest loading rate (0.03 mN s^{-1}) and that the pop-in size gradually decreases with the increase in the loading rate. At the highest loading rate of 300 mN s^{-1} pop-in events disappear. This observation is consistent with experiments performed on Pd-based and Mg-based bulk metallic glass [11]. Schuh et al. [11] proposed that the absence of pop-in events at high loading rates was caused by the kinetic limitation for the nucleation of shear bands and they also suggested the existence of a new homogeneous flow region. However, others have argued that it might just be a result of instrumental blurring at high loading rates [13].

In order to address the dispute on this strain rate effect, we carried out a study on the time duration of these pop-in events at different loading rates. The data acquisition rates and pop-in durations used in this study are listed in Table 1. The time resolution of the instrument was determined by the data acquisition rate. Since the total number of data points in each indentation test was fixed, a lower data acquisition rate was expected for the test with a lower loading rate. An event that is shorter than the acquisition time for a single datum point is considered immeasurable. As indicated in Table 1, for loading rates slower than 1 mN s^{-1} a pop-in event would be completed in a time

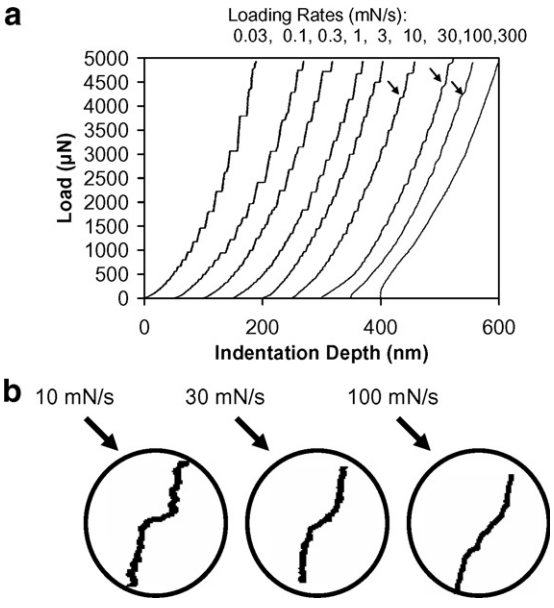

Fig. 3. Pop-in size variation with the loading rates during nanoindentation of an Au-based bulk metallic glass. (a) P–h curves at nine different loading rates and (b) typical pop-in step at high loading rates of 10, 30 and 100 mN s^{-1}.

Table 1
Summary of the data acquisition rates and pop-in durations at different loading rates during nanoindentation of Au-based bulk metallic glass at room temperature

Loading rate ($mN\ s^{-1}$)	Data acquisition rate (Hz)	Time duration between two data points (ms)	Average data points for a pop-in event at ~4 mN	Time duration for a pop-in event at ~4 mN (ms)
0.03	24.33	41.097	1	N/A
0.1	81.11	12.3	1	N/A
0.3	243.31	4.11	1	N/A
1	811.03	1.23	1	N/A
3	2433.09	0.411	3–4	1.46
10	8130.08	0.123	11	1.35
30	12048.19	0.083	16	1.33
100	10204.08	0.098	14	1.37
300	15384.62	0.065	N/A	N/A

period faster than the acquisition time for one datum point, meaning that the pop-in event cannot be fully captured by the instrument. In contrast, for loading rates of 3 $mN\ s^{-1}$ and higher, more than two data points were recorded during each pop-in duration and the pop-in time was determined as ~1.4 ms independent of the loading rates. Thus, at high loading rates where the load increment in 1.4 ms cannot be neglected, *P–h* curves with different slopes were observed instead of horizontal lines within each pop-in duration, as shown in Fig. 3b. The pop-in slopes increased with loading rates from 10 to 100 $mN\ s^{-1}$. At the maximum loading rate of 300 $mN\ s^{-1}$, the pop-in slope is, in principle, three times as high as that of 100 $mN\ s^{-1}$: this becomes similar to the elastic slope of the *P–h* curve in the absence of the pop-in event and cannot be readily distinguished. From these observations we concluded that, with the present instrument, pop-in events would not be distinguished from *P–h* curves when using loading rates higher than 300 $mN\ s^{-1}$. However, this does not mean that pop-in events disappear above 300 $mN\ s^{-1}$, but neither does it provide direct evidence to support a new homogeneous flow region at high strain rates.

In the free-volume theory [18–20] the strain rate of bulk metallic glass is determined by a combination of applied stress, temperature and free-volume accumulations, as described in the following equation [18–20]:

$$\dot{\varepsilon} = 2\alpha \exp\left(-\frac{\gamma v^*}{v_f}\right)\left(\frac{\varepsilon_0 v_0}{\Omega}\right) J \exp\left(-\frac{\Delta G^m}{kT}\right) \sinh\left(\frac{\varepsilon_0 v_0 \sigma}{2kT}\right) \quad (5)$$

where $\dot{\varepsilon}$ is the strain rate, α is the volume fraction of the flow units, γ is a geometrical factor between 1.0 and 0.5 v^* is the effective hard-sphere size of the atom, v_f is the average free volume of an atom, ε_0 is the strain of a flow unit, v_0 is the volume of a flow unit, Ω is the atomic volume, J is the atomic vibration frequency, ΔG^m is the thermal activation energy, k is the Boltzmann constant, T is the temperature and σ is the applied stress.

In the situation when temperature and stress/hardness are fixed $\ln(\dot{\varepsilon}) - A = -\frac{\gamma v^*}{v_f}$, where $A = \ln\left(2\alpha J \frac{\varepsilon_0 v_0}{\Omega} \sinh\left(\frac{\varepsilon_0 v_0 \sigma}{2kT}\right)\right) - \frac{\Delta G^m}{kT}$ is a constant. Let us assume that the number of shear band nucleation sites is proportional to the free volume density, i.e. $[\ln(\dot{\varepsilon}) - A] \propto -\frac{1}{N}$, where N is the number of sites for shear band nucleation. It is also reasonable to assume that the number of pop-in events N_p is proportional to the number of shear bands, if not the same. During nanoindentation the total plastic displacement is $h_p = N_p \Delta h'$, where $\Delta h'$ is the average pop-in displacement for all indentation depths. According to Eq. (4), $\Delta h'$ is proportional to the hardness serration ΔH. In the present study, a constant hardness value of 3.9 GPa was observed for the Au-bulk metallic glass independent of the loading/strain rates. Thus, h_p can be considered as a constant at different strain rates. With these assumptions, the strain rate can be correlated to the pop-in size as

$$[\ln(\dot{\varepsilon}) - A] \propto -\frac{1}{N_p} \propto -\frac{\Delta h'}{h_p} \propto -\Delta h' \propto -\Delta H \quad (6)$$

From Eq. (6) we predict that the hardness serration (or pop-in size) should decrease with the logarithmic increase in the strain rate. To verify this prediction, the *P–h* curves in Fig. 3a were projected into hardness serration curves in Fig. 4a. A decrease in the size of the hardness serration with increasing strain rate is clearly observed. Note that, in Fig. 4a, the loading rates were converted into strain rates following the same procedures described in Refs. [11,12]. In addition, the *P–h* curves with loading rates above 100 $mN\ s^{-1}$ (strain rate >4.6 s^{-1}) were not included in Fig. 4a because the pop-in steps were largely distorted. In order to quantify the size of the hardness serration further, nine indentation tests were performed at each strain rate. A computer filter program selected the hardness maxima and minima in each curve and the size of the hardness serration for each curve was then calculated as the difference between the average maximum and minimum values. The hardness serration as a function of the logarithmic strain rate is plotted in Fig. 4b.

It is evident in this figure that the hardness serration decreases linearly with the logarithmic increase in the strain rates, which is consistent with the theoretical prediction in Eq. (6). It is particularly notable in Fig. 4b that the serration size curve intercepts the strain rate axis ($\Delta H = 0$) at a very high strain rate (1700 s^{-1}). This is the strain rate beyond which, in theory, no discrete emission of shear band would occur, i.e. the new homogeneous region described by Schuh et al. [11]. In other words, above this strain rate the entire bulk material would behave like a

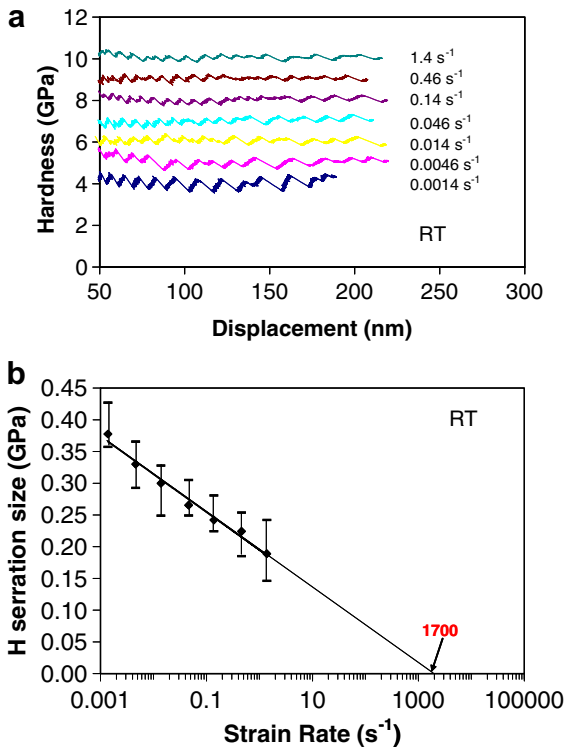

Fig. 4. The hardness serration size variation with the strain rates during nanoindentation of an Au-based bulk metallic glass at room temperature. (a) The hardness versus displacement at different strain rates and (b) the hardness serration size versus the strain rate.

large shear band under deformation. Intuitively, when the applied strain rate approaches a value that corresponds to the localized stain rate within shear bands, the entire material will have to be under shear banding in order to accommodate the applied strain rate. However, this strain rate is much higher than that can be achieved using the present instrument and is well in the range of the predicted strain rate for a shear band [11].

Schuh et al. [11] proposed that shear banding in a glass is governed by the shear band nucleation not its propagation and there exists a critical nucleant size beyond which a shear band is able to propagate catastrophically:

$$N_s = \frac{N_0 J_0 \varepsilon_n}{\dot{\varepsilon}^*} \tag{7}$$

where N_s is the number of atoms contained in a shear band nucleant, $N_0 \approx 30$ [19] is the number of atoms in a basic flow unit, which is also known as the shear transition zone, $J_0 \approx 10^{12}$ [19] is the natural vibration frequency of a shear transition zone, $\varepsilon_n \approx 1.7 \times 10^{-4}$ (read from Fig. 8 in Ref. [11] at $T/T_g = 0.75$) is the shear band nucleation strain and $\dot{\varepsilon}^* = 1700\ s^{-1}$ is the threshold strain rate for homogenous shear banding (Fig. 4b). The size of a shear band nucleant can thus be estimated from Eq. (7) as 3×10^6 atoms or a sphere of ~30 nm in diameter (the atomic size of gold is ~0.2 nm). This size agrees reasonably with the shear band thickness of 10–20 nm [24,25].

4. Conclusion

The mechanical properties of an $Au_{49}Ag_{5.5}Pd_{2.3}Cu_{26.9}Si_{16.3}$ bulk metallic glass were characterized by nanoindentation with a strain rate variation of up to four orders of magnitude. The shear band pop-in events were analyzed in detail at different loads and strain rates.

- Every pop-in event was accompanied by a constant hardness reduction, independent of the applied load, suggesting that the shear band was arrested by a constant stress reduction, which, in turn, was caused by an increase in the average free volume inside the shear band. This observation led to the conclusion that the size of a pop-in event should follow a linear relationship with the indentation depth and this was consistent with the experimental observations.
- We concluded from a free-volume model that the hardness serration caused by a pop-in event should linearly decrease with the logarithmic increase in the strain rate. The relationship was verified by experiments conducted over a wide range of strain rates. The data also indicated the existence of a critical strain rate of $\sim 1.7 \times 10^3\ s^{-1}$ for a second homogeneous flow region. This critical strain rate compared well with the expected strain rate for localized shear banding. Using the value of the critical strain rate, we further estimated the size of nuclei for shear banding and found it was similar to the width of the shear bands reported in the literature.

Acknowledgements

The Division of Materials Sciences and Engineering, Office of Basic Energy Sciences, US Department of Energy supported this work under contract DE-FG02-06ER46338 with the University of Tennessee. The authors are grateful to Ms. Laura Riester for her help in operating the nanoindentation instrument at the High Temperature Materials Laboratory, Oak Ridge National Laboratory.

References

[1] Cahn RW. Nature 1989;341:183.
[2] Greer AL. Science 1995;267:1947.
[3] Liu CT, Heatherly L, Easton DS, Carmichael CA, Schneibel JH, Chen CH, et al. Metall Mater Trans A 1998;29(7):1811.
[4] Johnson WL. MRS Bull 1999;24(10):42.
[5] Lewandowski JJ, Wang WH, Greer AL. Phil Mag Lett 2005;85(2):77.
[6] Das J, Tang MB, Kim KB. Phys Rev Lett 2005;94(20):205501.
[7] Bei H, Xie S, George EP. Phys Rev Lett 2006;96(10):105503.
[8] Jiang WH, Liaw PK. unpublished data.
[9] Yang B, Morrison ML, Liaw PK, Liu CT, Buchanan RA, Wang G, et al. Appl Phys Lett 2005;86:141904.
[10] Yang B, Nieh TG, Morrison ML, Liaw PK, Liu CT, Buchanan RA, et al. J Mater Res 2006;21:915.
[11] Schuh CA, Lund AC, Nieh TG. Acta Mater 2004;52:5879.
[12] Schuh CA, Nieh TG. Acta Mater 2003;51:87.

[13] Greer AL, Castellero A, Madge SV, Walker IT, Wilde JR. Mater Sci Eng A 2004;375:1182.
[14] Schroers J, Lohwongwatana B, Johnson WL, Peker A. Appl Phys Lett 2005;87:061912.
[15] Wright WJ, Saha R, Nix WD. Mater Trans 2001;42:642.
[16] Golovin YI, Ivolgin VI, Khonik VA, Kitagawa K, Tyurin AI. Scripta Mater 2001;45:947.
[17] Kovacs Z, Castellero A, Greer AL, Lendvai J, Baricco M. Mater Sci Eng A 2004;387:1012.
[18] Spaepen F. Acta Mater 1977;25:407.
[19] Argon AS. Acta Mater 1978;27:47.
[20] Spaepen F. Scripta Mater 2006;54:363.
[21] Jiang WH, Pinkerton FE, Atzmon M. Acta Mater 2005;53:3469.
[22] Oliver WC, Pharr GM. J Mater Res 1992;7:1564.
[23] Hainsworth SV, Chandler HW, Page TF. J Mater Res 1995;11: 1987.
[24] Pekarskaya E, Kim CP, Johnson WL. J Mater Res 2001;16:2513.
[25] Donovan PE, Stobbs WM. Acta Metall 1981;29:1419.